Energy 321 (2025) 135391

Contents lists available at ScienceDirect

Energy

journal homepage: www.elsevier.com/locate/energy

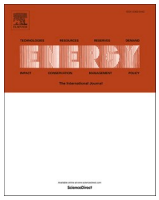

Experimental investigation on the effect of iron-rich coal ash on biomass-volatile combustion characteristics in the fluidized bed

Changhao Ma [a,b], Haoyu Tian [c], Yuchen Ma [a], Bingjun Du [a,b], Yang Zhang [a,b,d], Junfu Lyu [a,b,d], Xiwei Ke [b,d,*]

[a] Key Laboratory for Thermal Science and Power Engineering of Ministry of Education, Department of Energy and Power Engineering, Tsinghua University, Beijing 100084, China
[b] Shanxi Research Institute of Huairou Laboratory, Taiyuan 030032, China
[c] Department of Chemical and Biological Engineering, The Hong Kong University of Science and Technology, Clear Water Bay, Kowloon, Hong Kong Special Administrative Region of China
[d] Beijing Huairou Laboratory, Beijing 101499, China

ARTICLE INFO

Keywords:
Biomass volatile
Fluidized bed combustion
Alternative bed material
NO_x emission

ABSTRACT

The adoption of alternative bed material may effectively address issues in the biomass-fired circulating fluidized bed (CFB) boiler, such as uneven fuel-oxygen mixing and low combustion efficiency. This study presents a novel additive, iron-rich coal ash, which is expected to enhance the combustion performance of biomass-fired CFB boilers while may affect the transformation mechanism of volatiles and nitrogen oxides. In this paper, the Indonesian lignite ash was applied as the active bed material to test its effect on the combustion characteristics of volatiles yield from biomass in a lab-scale bubbling fluidized bed. Experimental results indicate that the addition of iron-rich lignite ash (54.4 % Fe_2O_3) can evidently improve the oxidation of volatiles, which is comparable to steel slag and ilmenite. By contrast, the other two bituminous coal ashes show weaker reactivity. Through composition analysis, the effect of alternative bed material is positively correlated with the iron content. In addition, increasing the additive substitution ratio can promote volatile combustion, but tends to saturate after reaching 50 %. Although reducing the particle size exhibits poorer mass transfer in bed, smaller ash particles can provide more reactive surface areas, thus the conversion rate of volatiles increases. A substitution ratio of 50 % and a bed material size of 150–200 μm are suitable options. Besides, with increasing temperature and excess oxygen coefficient, the combustion of volatile becomes more complete. However, for all cases, as combustion efficiency improves, there is an increase in NO_x emission. That means the addition of iron-rich coal ash may bring negative effect in the NO_x emission control, which should be noticed in the industrial application. In conclusion, this work offers important engineering recommendations for the large-scale utilization of solid waste coal ash and the enhancement of conversion efficiency in biomass-fired CFB boilers.

1. Introduction

The escalating energy crisis and growing environmental concerns have drawn increasing attention in recent years. The goal of achieving carbon neutrality by 2060 has introduced new demands for the adjustment of energy structure in China [1]. Biomass, as an environmentally friendly, low-cost and carbon-neutral renewable energy source, can be utilized as a fuel for combustion in boilers, which holds significant potential for meeting carbon emission control policy [2]. Additionally, biomass-fired boilers offer the same dispatchability as the traditional thermal power units, thus facilitating the accommodation of wind or photovoltaic power generation. Consequently, biomass is expected to play a crucial role in the power systems with an increasing share of new energy sources [3,4].

Currently, biomass combustion predominantly utilizes grate furnaces or pulverized coal boilers. However, they may be restricted by combustion efficiency or economic property when burning biomass. Compared with grate furnaces and pulverized coal boilers, circulating fluidized bed (CFB) combustion technology is particularly noteworthy due to its broad fuel adaptability and low cost in pollutant emission control. These characteristics make the CFB boiler suitable for biomass fuels, which have low energy density, high moisture content, irregular

* Corresponding author. Shanxi Research Institute of Huairou Laboratory, Taiyuan 030032, China.
E-mail address: kexiwei@sxri.hrl.ac.cn (X. Ke).

https://doi.org/10.1016/j.energy.2025.135391
Received 14 November 2024; Received in revised form 1 February 2025; Accepted 1 March 2025
Available online 1 March 2025
0360-5442/

shape and a wide range of particle size [5,6].

However, the biomass-fired CFB boiler currently faces several significant challenges [7]. Most biomass is rich in alkali metals and chlorine, leading to severe slagging, fouling and corrosion on heating surfaces, as well as bed material agglomeration [8], which restricts the improvement of boiler steam parameters. Furthermore, the rapid release of volatiles from biomass, coupled with the intermittent feeding of biomass fuels and uneven spatial distribution of fuel particles, leads to inconsistency between the timescales of chemical reactions and diffusion. This results in inadequate mixing of fuel and oxygen, thereby reducing combustion efficiency [9]. To achieve complete combustion, a relatively high excess air coefficient is often applied. Nevertheless, the formation of flame during volatiles combustion (high temperature in local areas) and the low inventory of reducing char can contribute to high NO_x emission [10].

Recent research suggests that employing alternative bed material can effectively address these issues in biomass-fired CFB boilers [11–14]. For instance, additive particles can capture alkali metals such as potassium (K) and sodium (Na), which are prone to causing slagging in biomass fuels. Through a series of chemical reactions, these alkali metals are converted into high-melting-point compounds [15,16]. In addition, when oxygen carriers are used as alternative bed material, they undergo continuous oxidation-reduction cycles when moving between different atmospheric regions, thereby facilitating oxygen transport [17]. Oxygen carrier aided combustion (OCAC) enhances the mixing between the fuel and the oxygen [12,18,19]. Moreover, certain alternative bed material can influence the conversion processes of nitrogen oxides [20–22].

Current selection of alternative bed materials primarily focuses on natural minerals and industrial waste products [23,24]. The utilization of kaolin, zeolite, or other inexpensive minerals and solid wastes can alleviate slagging, fouling, and corrosion happened on heating surfaces [25–29]. Some studies also have shown that substituting part or all of the bed materials with ilmenite, manganese ore, or steel slag results in increasingly uniform temperature distribution, more complete fuel combustion, and a significant reduction in CO emissions at the outlet [30–32]. Additionally, iron-based materials have gained attention for their influence on NO_x conversion [33,34]. Previous research has reported that these materials inhibit the conversion of NO_x precursors (HCN and NH_3) into NO [35,36]. Simultaneously, generated NO can be reduced to N_2 by the heterogeneous reaction on iron particle surface [37]. However, other studies have also indicated that iron-based material may have an inhibitory effect on SNCR efficiency, especially under aerobic and low-temperature conditions, where it may catalyze more NH_3 oxidation to generate NO_x [38].

Currently, most OCAC additives use iron contained solid particles as the primary active components [39]. In fact, iron-based oxygen carriers have attracted considerable interest in chemical looping combustion due to their low cost, high redox activity and mechanical strength [40]. In addition to natural minerals like ilmenite, another high-iron content material iron-rich coal ash has been largely overlooked, which could potentially serve as an ideal alternative bed material for fluidized bed combustion. Previous research on the role of coal ash in biomass-fired fluidized bed predominantly focuses on mitigating fouling and corrosion on heat transfer surfaces, with limited exploration into the relationship between coal ash and biomass volatile combustion.

Compared to other bed materials, iron-rich coal ash possesses the following advantages. To begin with, coal ash is widely available and low-cost. Coal-fired power plants generate substantial amounts of coal ash daily, making its disposal a growing concern [41]. Applying coal ash as an alternative bed material in biomass-fired CFB boilers also presents an environmentally friendly solution for large quantities of solid waste, thereby achieving a dual benefit of economic and environmental advantages. For further analysis, the particle size of coal ash (ranging from 10 μm to 500 μm) is suitable, with good abrasion resistance, allowing it to participate in long-term material circulation. Additionally, the continuous scouring by the circulating coal ash particles can effectively impede the formation and growth of slagging layer, thereby reducing the corrosion rate of high temperature heating surface arranged inside the boiler furnace [42]. Besides, it is typically rich in minerals such as aluminum (Al), calcium (Ca), or magnesium (Mg), which have been shown to form high-melting-point alkali metal compounds that can significantly mitigate corrosion and slagging issues [43]. In addition to its potential oxygen-carrying function, research has demonstrated that iron-rich coal ash exhibits significant effects on NO reduction owing to its iron content [44,45]. However, the influence of iron-rich coal ash on the combustion and emission characteristics of biomass-fired CFB boilers remains underexplored.

This study constructed a lab-scale bubbling fluidized bed experimental system to explore if the addition of coal ash can significantly affect the combustion performance of simulated biomass volatiles. Three types of coal ash, obtained from one Indonesian lignite and two Chinese bituminous coals, were applied as the research objectives. Meanwhile, silica sand, ilmenite and steel slag were also used as the reference samples. In addition, the effects of some operation conditions such as additive substitution ratio and bed material size on the volatile combustion characteristics were also discussed.

2. Methods

2.1. Experimental system and procedure

The bubbling fluidized bed experimental system, as illustrated in Fig. 1, was divided into three main parts: the gas distribution system, the reactor and heating system, and the gas detection system.

The experimental reaction was conducted inside the customized vertical glass reaction tube, which is 1209 mm in height. The inner diameter of the tube is 40 mm, with 2 mm thick walls. The gas inlets are 10 mm in diameter, and the outlet at the top is 20 mm in diameter. A quartz sintered plate gas distributor with a thickness of 5 mm is installed on the middle of the tube, 580 mm in height from the bottom. The chamber below the gas distributor serves the function of preheating gases, which is filled with quartz glass fragments. The reactor is externally heated with an electric heating system, and the height of heating zone is 465 mm. Two K-type thermocouples are employed: one is connected to the reactor temperature controller to achieve precise temperature regulation, while the other is connected to display instrument for real-time monitoring and recording of the bed temperature.

To prevent the oxidizing gas from contacting the reducing gas before entering the bed, the gas supply was divided into two streams. A mixture of oxygen and argon, in a predetermined proportion, was introduced from the bottom of the reaction tube, while synthesized volatiles (NH_3, CH_4, CO, CO_2, H_2) were introduced through a side inlet of the reaction tube. Note that the alkaline NH_3 and the acidic CO_2 could not be stored in the same gas cylinder to prevent the formation of $(NH_4)_2CO_3$ or NH_4HCO_3. Therefore, they were supplied independently through a gas cylinder containing three components (CO, CO_2, H_2) and another gas cylinder containing two components (NH_3, CH_4).

All gases passed through the gas distribution plate to fluidize the bed and undergo reactions. Before entering the detection equipment, the exhaust gas passed through a condenser in the pipeline to cool the water vapor generated during the reaction process, preventing adverse effects on subsequent detection. Additionally, a filter was installed to protect the detection equipment from potential damage. A gas analyzer (Testo 350) was applied to test and record the composition of flue gas flowing out of the bubbling bed reactor. One thing should be pointed out that, the CO concentration at the reactor outlet exceeds the measurement upper limit of the detection device (5000 ppm) under conditions of low excess oxygen coefficient, which was not shown in the results.

Bed materials were added into the reactor through a funnel, and the static bed height was recorded. Argon was introduced at a flow rate of 0.5 L/min to initiate heating. Once reaching the preset operating temperature, the reaction gases were introduced. The mass flow controllers

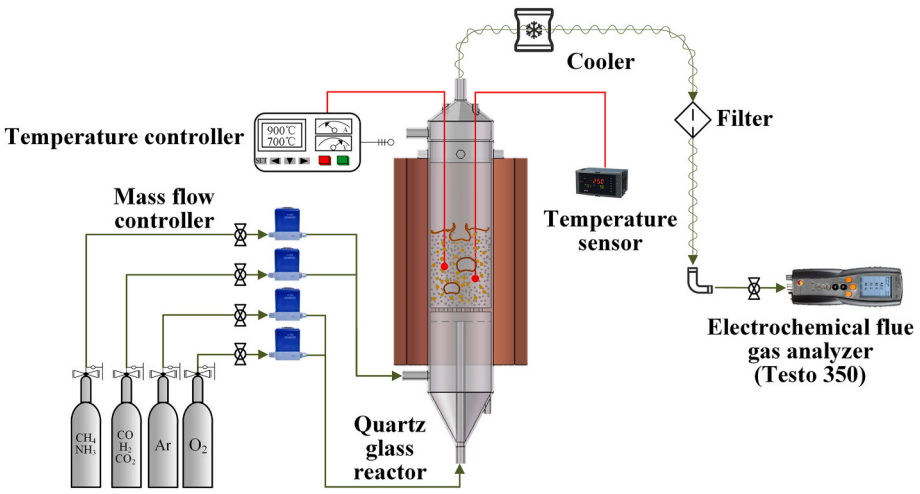

Fig. 1. Schematic diagram of experimental device.

(MFC) were adjusted sequentially for argon, NH_3+CH_4, CO + CO_2+H_2, and O_2 in the gas order. After that, the concentrations of O_2, CO_2, and NO_x (NO and NO_2) were recorded when the gas analyzer readings stabilized.

When completing all tests, the MFCs were closed sequentially in the gas order of O_2, CO + CO_2+H_2, and NH_3+CH_4, while the argon remained flowing through the reactor tube. The furnace was then shut down and allowed to cool naturally. After the bed temperature dropped to room temperature, the argon supply was stopped.

2.2. Experimental material and operating conditions

The active particles primarily influence volatile gas combustion and nitrogen oxide conversion behavior through gas-solid reactions, with minimal direct effect on biomass pyrolysis and char conversion processes. In addition, most agricultural and forestry biomass has a volatile content exceeding 60 %, with a relatively low char content. Consequently, some researchers have applied volatile components such as methane as model fuels to study the impact of alternative bed material on biomass fluidized bed combustion [11]. In this study, the composition of the synthesized volatile (18.8 % H_2, 27.7 % CH_4, 26.9 % CO, 25.9 % CO_2, 0.7 % NH_3) was determined through an analysis of the straw pyrolysis products. According to this result, the concentration of each component at the reactor inlet was set as 34840 ppm (H_2), 51427 ppm (CH_4), 50000 ppm (CO), 48138 ppm (CO_2) and 1319 ppm (NH_3), respectively.

Under the basic experimental condition, silica sand was used as the primary bed material, with Indonesian lignite ash applied as alternative bed material. The bed material size was 150–180 μm, with a total mass of 60 g, and the substitution ratio was 20 %. In addition, the study aimed to investigate the effects of alternative bed material type, substitution ratio, bed material size, temperature and excess oxygen coefficient on the combustion characteristics of volatiles. The experimental conditions are summarized in Table 1.

When exploring the effect of alternative bed material type, three coal ash samples, Indonesian lignite ash, Jiaocheng bituminous coal ash and Shuozhou bituminous coal ash, were selected as the main research objectives. These samples are all derived from commonly used thermal coals in power plants, rather than coals intended for chemical applications. Indonesian lignite is among the most traded coal types globally, with extensive exports to Southeast Asia and East Asia. The other two types of bituminous coal are sourced from Shanxi province in China. The proximate and ultimate analysis results of the relevant three types of coal are listed in Table 2. The ash content of Indonesian lignite is relatively low (2.6 %), while the volatile content reaches 34.93 %, higher than other two types of bituminous coal. Ilmenite and steel slag were also used as comparison. XRF analysis was conducted for these alternative bed materials and Fig. 2 presents the mass fractions of different elemental oxides in these additives. The main components include silicon dioxide, aluminum oxide, calcium oxide, iron oxide and magnesium oxide. Among three types of coal ash, the Fe_2O_3 content in Indonesian lignite ash (54.4 %) was significantly higher than those in Shuozhou coal ash (8.82 %) and Jiaocheng coal ash (12.47 %), and was comparable to the Fe_2O_3 content in ilmenite and steel slag.

Malvern laser particle size analysis was conducted on Indonesian lignite ash under different particle sizes. The particle size distribution results are shown in Fig. 3, which approximately follows a normal distribution within their respective size ranges, consistent with the

Table 1
Experimental conditions.

Number	Alternative bed material type	Temperature/°C	Excess oxygen coefficient/-	Bed material size/μm	Substitution ratio/%
1	Indonesian lignite ash	700/750/800/850/900	1.3–2	150–180	20 50 75 100
2	Indonesian lignite ash	700/750/800/850/900	1.3–2	105–125 125–150 200–250 250–300	20
3	Jiaocheng coal ash	700/750/800/850/900	1.5–2	150–180	20
4	Shuozhou coal ash		1.5–2		
5	Ilmenite		1.3–2		
6	Steel slag		1.3–2		
7	Silica sand		1.5–2		

Table 2
Proximate and ultimate analysis results of three types of coal.

Coal	Proximate analysis/%				Ultimate analysis/%				
	M_{ar}	A_{ar}	V_{ar}	FC_{ar}	C_{ar}	H_{ar}	O_{ar}	N_{ar}	S_{ar}
Indonesian lignite	32.43	2.6	34.93	30.04	47.5	3.72	13.23	0.41	0.09
Coal	Proximate analysis/%				Ultimate analysis/%				
	M	A_d	V_d	FC_d	C_d	H_d	O_d	N_d	S_d
Jiaocheng bituminous coal	/	44.45	10.86	44.69	46.71	2.21	4.13	0.70	1.79
Shuozhou bituminous coal	/	38.14	24.97	36.89	47.96	3.19	8.79	0.85	1.07

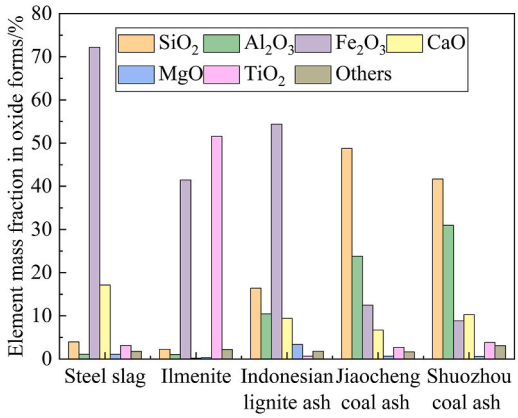

Fig. 2. XRF analysis results of different types of alternative bed materials (element mass fraction in oxide forms).

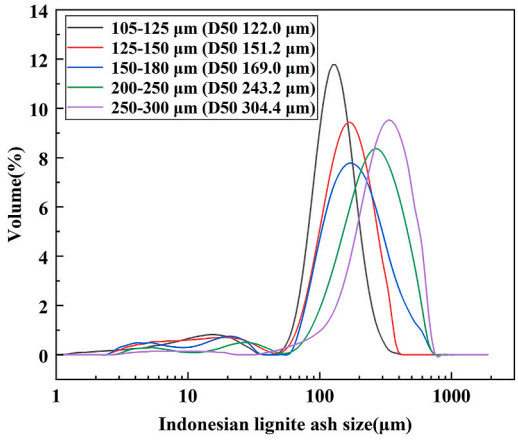

Fig. 3. Laser particle size analysis results of Indonesian lignite ash under different particle sizes.

anticipated results.

It was necessary to keep the gas flow rate inside the tube constant at 0.08 m/s under different temperature/oxygen conditions, ensuring consistent residence time of the gas in the reactor (about 2.13 s, from gas distributor to the top of heating zone). Therefore, the total flow rate at the reactor inlet should be adjusted according to different temperature conditions. The flow rate of each gas was determined by Eqs. (1)–(3).

$$Q_{inlet} = 60AvT_{cold}/1000T_{hot} \quad (1)$$

$$Q_{O_2,in} = \alpha\left(0.5Q_{CO,in} + 2Q_{CH_4,in} + 0.5Q_{H_2,in} + 1.25Q_{NH_3,in}\right) \quad (2)$$

$$Q_{Ar,in} = Q_{inlet} - \left(Q_{O_2,in} + Q_{CO,in} + Q_{CH_4,in} + Q_{CO_2,in} + Q_{H_2,in} + Q_{NH_3,in}\right) \quad (3)$$

where Q_{inlet} (L·min^{-1}) is the total gas flow rate at the inlet, A (m^2) is the tube cross-sectional area, v (m·s^{-1}) is the gas velocity in the tube, T_{hot} and T_{cold} (K) are the reaction and room temperature, respectively. $Q_{O2,in}$, $Q_{CO,in}$, $Q_{CH4,in}$, $Q_{CO2,in}$, $Q_{H2,in}$, $Q_{NH3,in}$, and $Q_{Ar,in}$ (L·min^{-1}) are the flow rate of O_2, CO, CH_4, CO_2, H_2, NH_3 and Ar at the reactor inlet, respectively, and α is the excess oxygen coefficient.

Given CO and NH_3 flow rate at the reactor inlet, and assuming complete combustion of the volatiles (proved by the CO concentration at the outlet), the flue gas flow rate at the reactor outlet can be calculated. Combined with the gas concentrations from the analyzer at the outlet, the CO conversion rate (X_{CO}) and NH_3 to NO_x conversion rate ($X_{NH3\text{-}NO}$) was determined by Eqs. (4) and (5).

$$X_{CO} = \left(Q_{CO,in} - Q_{out}C_{CO,out}\right) / Q_{CO,in} \times 100\% \quad (4)$$

$$X_{NH_3-NO} = \left(Q_{NH_3,in} - Q_{out}C_{NO,out}\right) / Q_{NH_3,in} \times 100\% \quad (5)$$

where Q_{out} (L·min^{-1}) is the flow rate of flue gas at reactor outlet, $C_{CO,out}$ and $C_{NO,out}$ are CO and NO concentrations at the outlet, respectively.

2.3. Reproducibility validation

In terms of partial experimental conditions, each case was repeated three times. For these repeated experiments, the NO_x concentration at the reactor outlet under different temperatures and excess oxygen coefficients are shown in Fig. 4.

It is observed that the concentrations of NO_x at the reactor outlet remain relatively consistent under the same operating condition. Except for cases where gas concentrations approach the lower detection limit of the measurement instrument, leading to reduced accuracy, the average deviation of NO_x concentrations at the outlet does not exceed 5 % under most conditions. This demonstrates the stability and reliability of the experimental system.

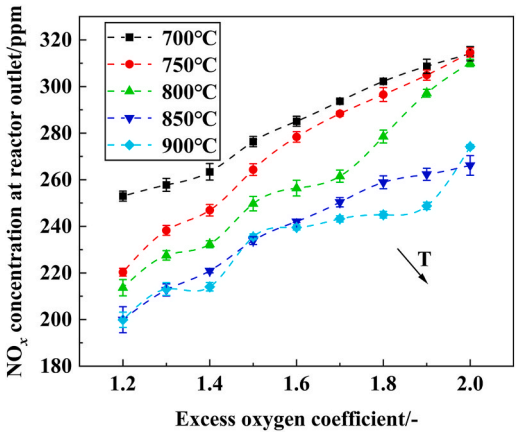

Fig. 4. NO_x concentration at the reactor outlet under different temperatures and excess oxygen coefficients (bed material size of 150–180 μm, substitution ratio of 20 %, Indonesian lignite ash as alternative bed material).

3. Results and discussion

3.1. Effect of alternative bed material type

Fig. 5 presents the variation in X_{CO}, O_2 concentration at reactor outlet ($C_{O2,\ out}$) and $X_{NH3\text{-}NO}$ when using different types of alternative bed materials.

From the analysis of Fig. 5, it can be observed that as the iron content in the alternative bed material increases, the O_2 concentration at reactor outlet gradually decreases, as well as the CO conversion rate increases. Specifically, when steel slag with highest Fe_2O_3 content (72.7 %) is used as the additive, the $C_{O2,\ out}$ reaches the lowest value among all cases (3.06 %). In contrast, for the reference group that using silica sand as the only bed material, the $C_{O2,\ out}$ is the highest (8.59 %).

Comparing the results of using three types of coal ash, when Indonesian lignite ash is applied as the alternative bed material, the conversion of volatile gas is the most sufficient (low O_2 concentration at the reactor outlet). Jiaocheng coal ash and Shuozhou coal ash, which have similar Fe_2O_3 content, exhibit comparable effect on volatile gas combustion. However, Jiaocheng coal ash leads to slightly higher X_{CO}, while Shuozhou coal ash results in a lower $C_{O2,\ out}$, which may be attributed to the discrepant catalytic/non-catalytic effect of ash to different gaseous species.

From the perspective of combustion performance, high iron content materials, including steel slag, ilmenite and Indonesian lignite ash, emerge as a promising alternative bed material [46]. On the one hand, Fe_2O_3 can participate in the oxidation reaction of CO, as shown in Eq. (6). On the other hand, iron-based materials can also serve as a catalyst for the CO oxidation [47]. Specifically, studies have suggested the potential mechanism that CO is first adsorbed onto the surface of Fe_2O_3, weakening an Fe-O bond. Subsequently, through compositional changes between FeO and Fe_2O_3, CO is oxidized to form CO_2 [44].

$$Fe_2O_3 + CO \rightarrow 2FeO + CO_2 \quad (6)$$

Nevertheless, the increasing iron content in the alternative bed material leads to a significant increase in NH_3 to NO_x conversion rate, as shown in Fig. 5. For instance, the $X_{NH3\text{-}NO}$ reaches to 19.31 % when adding steel slag to the bed material, which is much higher than that of the reference group (10.26 % for silica sand bed). Similarly, the iron-rich Indonesian lignite ash also promote the conversion of NH_3 to NO_x more evidently compared to the other two types of bituminous coal ash.

In certain cases, the addition of iron-based materials is beneficial for reducing NO_x emission [36,48,49]. Some publications pointed out that the effect of these active materials on the reduction of NO by CO (shown in Eq. (7)) and the decrease in oxygen content caused by the combustion-promoting effect both contribute to lower NO_x formation [44]. However, it should be noted that reaction in Eq. (7) is generally evident under oxygen-free conditions [50]. If a certain concentration of oxygen exits in the atmosphere, iron-containing compounds can also significantly catalyze the conversion of NH_3 into NO_x [51,52]. In terms of the experiments conducted in this work, the oxygen content in the outlet gas was above 3 %. Therefore, the reduction effect on NO_x may be not as significant as the promotion of NH_3 to NO_x conversion, demonstrating iron-based materials play a positive role in the formation of NO_x during the reaction.

$$CO + NO \xrightarrow{iron} CO_2 + 0.5N_2 \quad (7)$$

Moreover, as illustrated in the following content, experimental results under varying operational condition reveal that changes in factors favorable to combustion (higher additive substitution ratio and smaller bed material particle) lead to an increase in NO_x emission in nearly all cases. In summary, the effect of iron-rich coal ash on the biomass-volatile combustion is multifaceted, as it not only increases combustible gas conversion rate (which is beneficial to improve the boiler efficiency) but also generates more NO_x (disadvantage in pollutant emission control). Previous studies have highlighted the strong sensitivity of NO_x emissions to oxygen concentrations [53]. Meanwhile, since the addition of iron-rich coal ash can promote the combustion performance, a lower excess air coefficient can be applied to reduce the amount of NO_x emission [54].

3.2. Effect of additive substitution ratio

Fig. 6 illustrates the X_{CO}, $C_{O2,\ out}$ and $X_{NH3\text{-}NO}$ under different additive substitution ratios. It can be seen that when Indonesian lignite ash is applied as the alternative bed material, an increase in the substitution ratio leads to higher X_{CO} and $X_{NH3\text{-}NO}$, along with a reduction in $C_{O2,\ out}$. The enhanced conversion of biomass volatiles may result from the oxygen-carrying function and catalytic/non-catalytic reactivity effect of iron-rich coal ash, which can be investigated in further research.

Nevertheless, when the substitution ratio exceeds 50 %, the rate of change slows down, even unchanged, suggesting that further increases in the substitution ratio do not yield substantial benefits. Therefore, a saturation substitution ratio of active bed material (R_{sat}) exists. The cause of this phenomenon may be attributed to the finite active sites on the catalyst surface. CO temperature-programmed desorption (TPD)

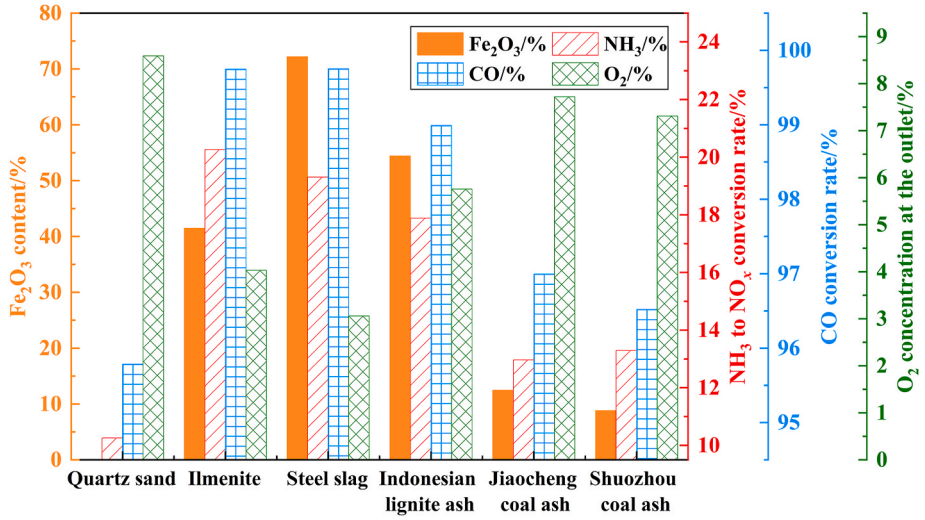

Fig. 5. Fe_2O_3 content of different types of alternative bed materials and their effects on combustion (temperature 800 °C, excess oxygen coefficient of 1.5, particle size of 150–180 μm, substitution ratio of 20 %).

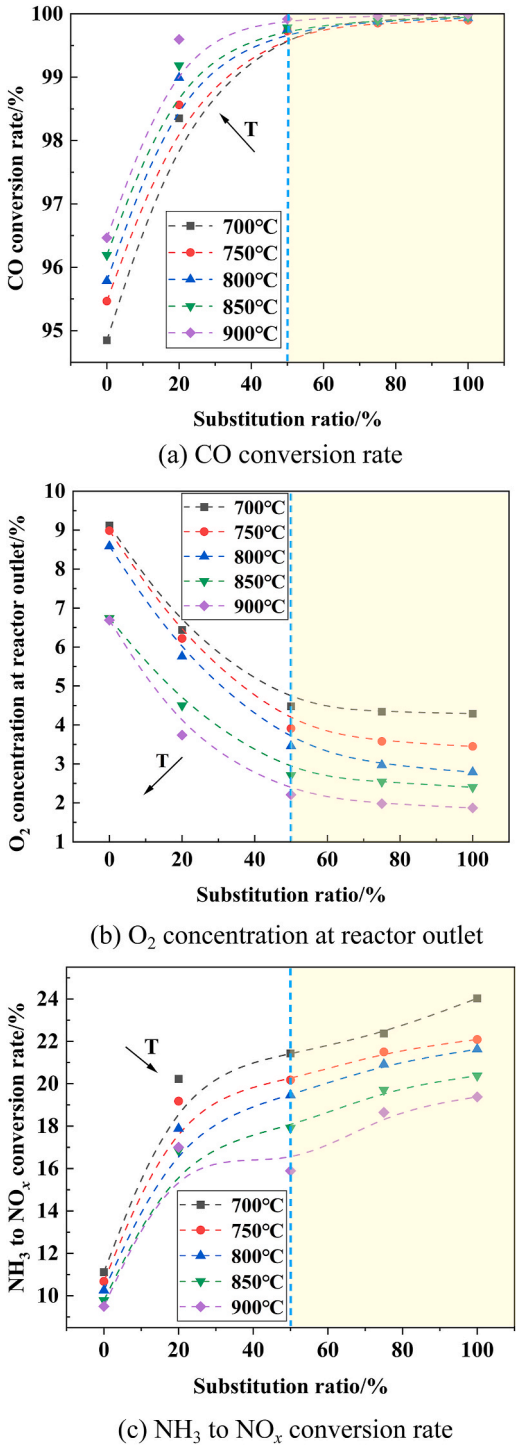

Fig. 6. Comparison of combustion results under different substitution ratios (excess oxygen coefficient of 1.5, bed particle size of 150–180 μm).

experiments were conducted on bed materials with different substitution ratios by using the chemical adsorption instrument (Micromeritics AutoChem II 2920). The experiments investigated the number of active surface sites, thus, reflecting the binding capacity between the bed material and the biomass volatiles. As shown in Fig. 7, both the peak intensity and desorption peak temperature gradually increase as the substitution ratio rises from 0 % to 50 %, indicating a stronger binding capacity between the bed material and CO. When the substitution ratio exceeds 50 %, the changes become not obvious. The differences in peak intensity between 50 % and 100 % substitution ratios are minimal.

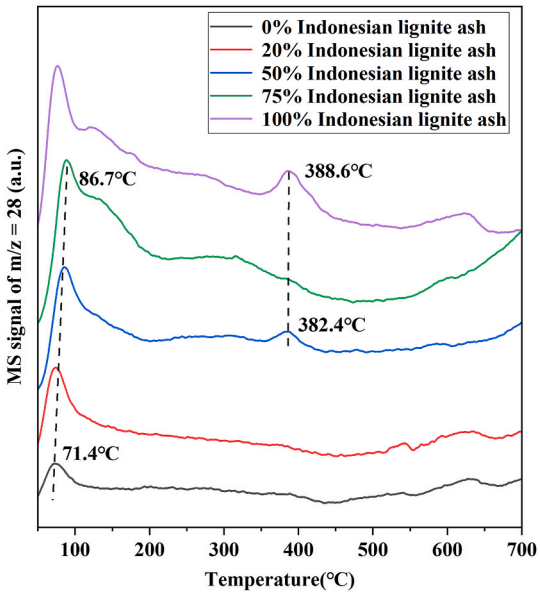

Fig. 7. CO temperature-programmed desorption (TPD) experiments results under different substitution ratios.

Additionally, absorption peaks appear at comparable temperatures (380–390 °C) for substitution ratios of 50 % and 100 %, suggesting that the surface states of the bed materials are similar at these ratios. Based on the above analysis, when the substitution ratio exceeds 50 %, the increase in binding capacity between the bed material and CO diminishes, which may explain the saturation of the effect.

Notably, the phenomenon of a saturated substitution ratio has also been observed in other studies. When ilmenite was employed as an active bed material, the enhancing effect on combustion reached a plateau after a substitution ratio of 50 % [18,55]. However, the saturation phenomenon was not clearly pronounced in the study where manganese ore (0–100 %) was used as an additive [54], indicating that the saturation phenomenon is also influenced by the type of additive employed. Additionally, it may also be related to the structure of the reactor. Limited gas residence time in the reactor prevents the increased active bed material from fully participating in the reaction. Besides, in this study, R_{sat} remains consistent (about 50 %) across different temperatures. It indicates that R_{sat} may have little relation to reaction activity, more likely correlated with residence time. Based on a comprehensive consideration of both the economic cost and the effectiveness of the active bed material, a substitution ratio of 50 % is identified as an optimal selection.

3.3. *Effect of bed material size*

Fig. 8 (a) and (b) show the X_{CO} and $C_{O2,\ out}$ under different bed materials' sizes, indicating that combustion is more complete when the bed material size is smaller. The BET surface area of lignite ash with different particle sizes are presented in Fig. 8 (d), showing a general decrease in surface area with an increase in bed material size. Smaller particle size leads to larger specific surface area, which provides more active sites for the reaction and facilitates the chemical reaction between biomass volatiles and oxygen on the particle surface.

Note that when the bed material size increases, the reaction surface area decreases exponentially, as shown in Fig. 9, indicating that the reaction effectiveness should also exhibit a similar trend. However, the results shown in Fig. 8 are quite opposite: as the bed material size decreases within relatively small size range, the gas concentrations at the reactor outlet vary slowly. This phenomenon indicates that another potential factor suppresses the effect of the active bed material on the volatile gas conversion as the bed material size decreases.

The particle size of bed material also has a significant impact on the gas-solid flow and mass transfer in bubbling fluidized bed reactors, which potentially influence the conversion results. Theoretical calculations and analysis are conducted to investigate the influence of bed material size on the gas-solid flow and mass transfer characteristics in the dense phase region of bubbling fluidized bed reactors. The calculation formulas are shown as Eqs. (8)–(10).

Gas phase volume fraction σ_B [56]:

$$\begin{cases} \sigma_B = 1/\left[1 + 1.3/\chi\left(\overline{U}_g - U_{mf}\right)^{-0.8}\right] \\ \chi = \left[0.26 + 0.70\exp\left(-3300 d_p\right)\right]\left(0.15 + \overline{U}_g - U_{mf}\right)^{-0.33} \end{cases} \tag{8}$$

where the subscripts B and E represent the bubble phase and the emulsion phase, respectively. $\overline{U}_g$ (m·s^{-1}) is the average gas velocity of the cross section, U_{mf} (m·s^{-1}) is the minimum fluidization velocity, and d_p (m) is the bed material size.

Interphase mass transfer coefficient $K_{g,B\leftrightarrow E}$ [57]:

$$K_{g,B\leftrightarrow E(i,m)} = \frac{U_{mf(i)}}{3} + \left(\frac{4 D_{g(i,m)} \varepsilon_{mf(i)} U_{g,B(i)}}{\pi d_{B(i)}}\right)^{1/2} \tag{9}$$

where D_g (m^2·s^{-1}) is the binary diffusion coefficient, ε_{mf} is the critical fluidization voidage, $U_{g,B}$ (m·s^{-1}) is the bubble rise velocity, and d_B (m) is the bubble diameter.

Mass transfer coefficient within the emulsion phase $K_{g,E}$ [58]:

$$\mathrm{Sh}_E = \frac{K_{g,E} d_p}{D_g} = 2\varepsilon_{mf} + 0.70\left(\frac{U_{mf} d_p \rho_g}{\mu_g \varepsilon_{mf}}\right)^{1/2}\left(\frac{\mu_g}{\rho_g D_g}\right)^{1/3} \tag{10}$$

where Sh_E is the sherwood number in the emulsion phase, ρ_g (kg·m^{-3}) is the average gas density, and μ_g (Pa·s) is the average gas viscosity.

Fig. 9 illustrates the variation of interphase mass transfer coefficient, mass transfer coefficient in the emulsion phase, gas phase volume fraction and total reaction surface area with bed material size, as calculated theoretically in the experimental range.

It can be observed that as the bed material size decreases, both the interphase mass transfer coefficient and mass transfer coefficient in the emulsion phase gradually decrease, indicating weakened mass transfer in the bed. Meanwhile, the gas phase volume fraction increases, suggesting that less gas in the bubble phase enters the emulsion phase and reaches the particle surface, thereby suppressing the effect of alternative bed material on the reaction. In summary, when the bed material size is below 200 μm, gas diffusion and mass transfer resistance in the bubbling bed dominate, thereby affecting the performance of the active bed material. Above a certain particle size, the reaction surface area (represents the reactivity of individual particles to some extent) becomes the predominant factor, outweighing the negative effect of mass transfer resistance.

In conclusion, an optimal granularity selection strategy is proposed primarily based on the following points. Firstly, as the bed material size decreases, the specific surface area increases, resulting in a larger active surface for catalysis. When the bed material particle size exceeds 200 μm, as shown in Fig. 8 (a), the conversion rate of CO significantly decreases. Therefore, the bed material size should not exceed 200 μm. Additionally, considering the wear of the active bed material in the fluidized bed, finer particles have a higher wear coefficient, which leads to the formation of fine ash that exits as fly ash, thereby losing its

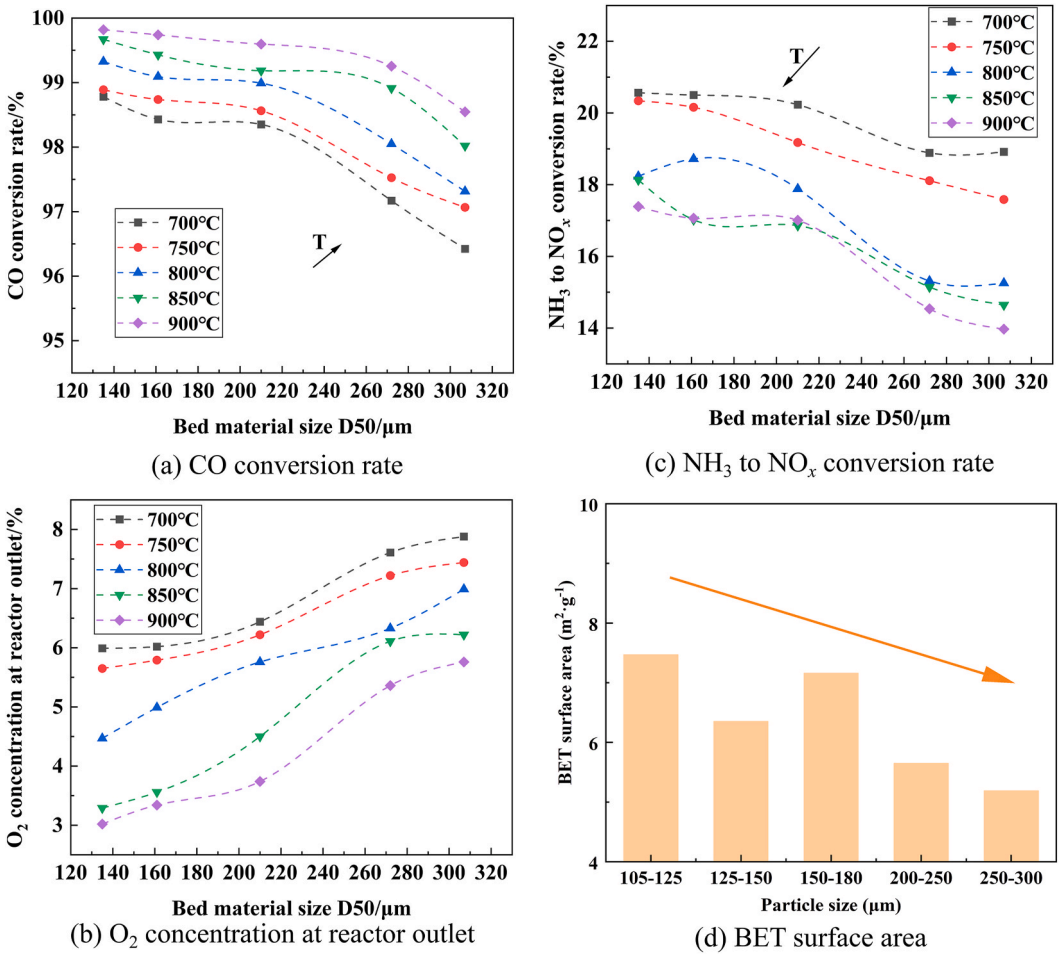

Fig. 8. Comparison of combustion results and BET surface area results under different particle sizes (excess oxygen coefficient of 1.5, substitution ratio of 20 %).

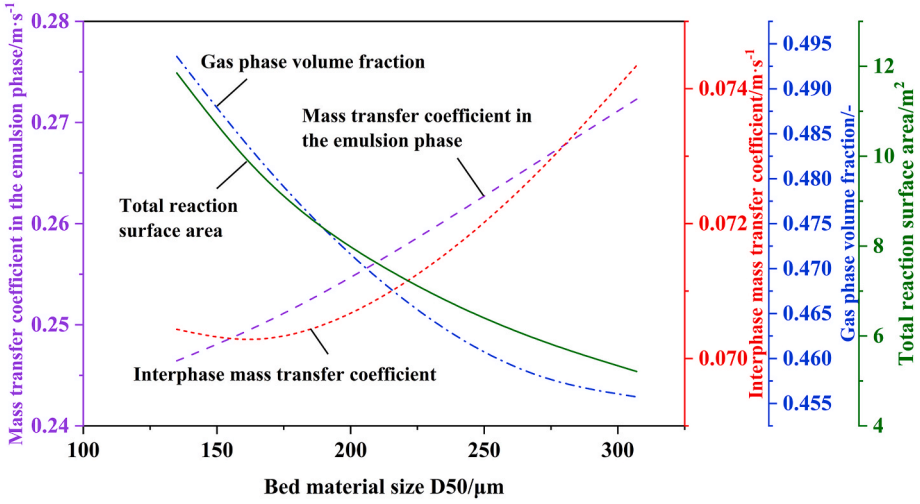

Fig. 9. Interphase mass transfer coefficient, mass transfer coefficient in the emulsion phase, gas phase volume fraction and total reaction surface area under different bed material sizes (reaction particle size 1 mm, temperature 800 °C, height 0.1 m, bed material mass 0.1 kg, bulk density 1500 kg·m^{-3}).

catalytic functionality [59]. Additionally, the catalytic effect of iron-rich coal ash on the reaction relies on the redox cycle in the fluidized bed, with the dense phase maintaining a reducing atmosphere and the dilute phase providing an oxidizing environment. In practical engineering applications, to form a well-established material circulation, the selection of bed material particle size must be moderate. Larger particles tend to deposit in the lower section and fail to participate in the circulation, while excessively fine particles exit as fly ash, resulting in an insufficient residence time. The most appropriate bed material size corresponds to the particle size of the circulating ash, with the median diameter of circulating ash typically ranging from 100 to 200 μm (depending on the efficiency of the separator). Therefore, a suitable particle size for the alternative bed material is identified in the range of 150–200 μm, which provides a valuable reference for practical engineering applications.

3.4. *Effect of temperature and excess oxygen coefficient*

The X_{CO} and $C_{O2,\ out}$ under different temperatures and excess oxygen coefficients are shown in Fig. 10. The results in Fig. 10 (a) show that as the temperature and excess oxygen coefficient increase, the X_{CO} increases, indicating more complete combustion.

In addition, the experimental data given in Fig. 11 (a) indicate that the reactive effect sensitivity of different types of alternative bed materials to temperature is relatively consistent. Nevertheless, as shown in Fig. 11 (b), Among three types of coal ash, Indonesian lignite ash exhibits weakest sensitivity to variations in the excess oxygen coefficient, while Jiaocheng coal ash and Shuozhou coal ash show stronger sensitivity. Once the excess oxygen coefficient exceeds 1.8, the biomass volatiles are essentially completely burned.

4. Conclusion

In this work, a potentially solid waste, iron-rich coal ash, was innovatively used as the alternative bed materials to explore its effect on the biomass volatile combustion characteristics in a bubbling fluidized bed. Some other common alternative bed materials such as steel slag and ilmenite were also tested as comparison. In addition, the influence of some important operational conditions such as additive substitution ratio, bed material size, temperature, and excess oxygen coefficient were investigated.

The effect of alternative bed material on the volatile gas conversion is positively correlated with their iron content. Among three types of coal ash, Indonesian lignite ash has the highest iron content and consequently exhibits most complete combustion. With the increase of

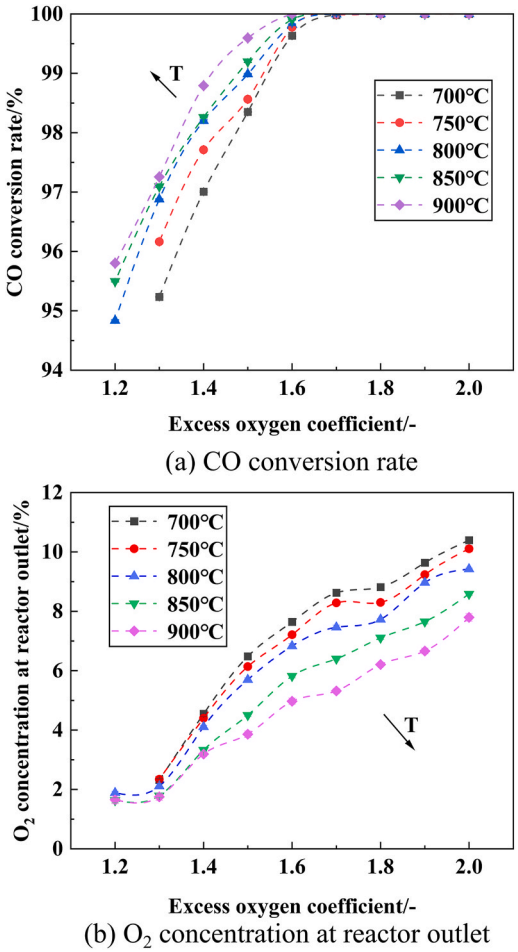

Fig. 10. Comparison of combustion results under different temperatures and excess oxygen coefficients (bed material size of 150–180 μm, substitution ratio of 20 %, Indonesian lignite ash as alternative bed material).

substitution ratio, the X_{CO} and $X_{NH3\text{-}NO}$ increase, however, such positive effect does not been further enhanced when the substitution ratio exceeds 50 %. In addition, if the bed material size is smaller, the active particles exhibit a larger surface area, resulting in higher reactivity and

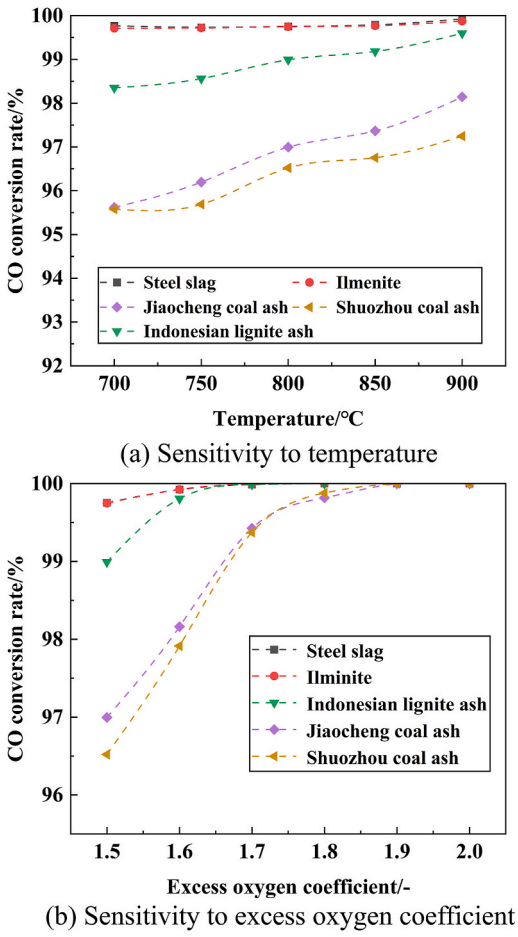

Fig. 11. Sensitivity of different alternative bed materials to temperature and excess oxygen coefficient (particle size of 150–180 μm, substitution ratio of 20 %).

more sufficient combustion. Nevertheless, theoretical calculations suggest that gas mass transfer resistance in the bubbling bed dominates the gas conversion process when the bed material size is below 200 μm. Besides, it should be noted that though the addition of iron-rich coal ash promotes the combustion efficiency, it also facilitates the conversion of NH_3 to NO_x. For this issue, a lower excess oxygen coefficient can be applied to reduce NO_x generation.

Based on the findings of this work, a novel and cost-effective kind of active materials suitable for OCAC technology is presented, which facilitates the efficient utilization of coal ash, a typical solid waste. Furthermore, this work offers important engineering recommendations for the application of iron-rich coal ash in biomass-fired CFB boilers, including optimal bed material particle size and additive substitution ratio. A substitution ratio of 50 % and a bed material size of 150–200 μm are suitable options. In subsequent research, full-loop simulations and pilot-scale experiment verification could be conducted to determine the optimal combination of operational conditions to enhance combustion efficiency while minimizing NO_x emission and other types of coal ash could be utilized to verify the general applicability. In addition, our subsequent research has demonstrated that Indonesian lignite ash exhibits remarkable redox properties. Further mechanism analysis on the effect of coal ash in enhancing volatile combustion and NO_x conversion is actively conducted and remains incomplete. Besides, the potential role of iron-rich coal ash in biomass pyrolysis and gasification at high temperatures is also a key direction for future research.

CRediT authorship contribution statement

Changhao Ma: Writing – original draft, Visualization, Validation, Methodology, Investigation, Formal analysis, Data curation. **Haoyu Tian:** Visualization, Validation, Methodology, Investigation, Formal analysis. **Yuchen Ma:** Writing – original draft, Validation, Investigation, Formal analysis. **Bingjun Du:** Visualization, Investigation. **Yang Zhang:** Supervision. **Junfu Lyu:** Supervision, Resources, Project administration, Funding acquisition. **Xiwei Ke:** Writing – review & editing, Supervision, Resources, Project administration, Funding acquisition, Conceptualization.

Declaration of competing interest

The authors declare that they have no known competing financial interests or personal relationships that could have appeared to influence the work reported in this paper.

Acknowledgements

This research was supported by the National Natural Science Foundation of China (52306251) and the Program of Beijing Huairou Laboratory (ZD2023008A).

Data availability

Data will be made available on request.

References

[1] Li H, Liu D, Yao D. Analysis and reflection on the development of power system towards the goal of carbon emission peak and carbon neutrality. Proc Chin Soc Electr Eng 2021;41:6245–58.
[2] Nunes LJR, Matias JCO, Catalao JPS. A review on torrefied biomass pellets as a sustainable alternative to coal in power generation. Renew Sustain Energy Rev 2014;40:153–60.
[3] Hansson J, Berndes G, Johnsson F, Kjarstad J. Co-firing biomass with coal for electricity generation-An assessment of the potential in EU27. Energy Policy 2009;37:1444–55.
[4] Demirbas A. Potential applications of renewable energy sources, biomass combustion problems in boiler power systems and combustion related environmental issues. Prog Energy Combust Sci 2005;31:171–92.
[5] Ke X, Jiang L, Lyu J, Yue G. Prospects for the low pollutant emission control of circulating fluidized bed combustion technology. Strategic Study of CAE 2021;23:120–8.
[6] Nielsen HP, Frandsen FJ, Dam-Johansen K, Baxter LL. The implications of chlorine-associated corrosion on the operation of biomass-fired boilers. Prog Energy Combust Sci 2000;26:283–98.
[7] Leckner B. Fluidized bed combustion: mixing and pollutant limitation. Prog Energy Combust Sci 1998;24:31–61.
[8] Salatino P, Solimene R. Mixing and segregation in fluidized bed thermochemical conversion of biomass. Powder Technol 2017;316:29–40.
[9] Niu YQ, Tan HZ, Hui SE. Ash-related issues during biomass combustion: alkali-induced slagging, silicate melt-induced slagging (ash fusion), agglomeration, corrosion, ash utilization, and related countermeasures. Prog Energy Combust Sci 2016;52:1–61.
[10] Williams A, Jones JM, Ma L, Pourkashanian M. Pollutants from the combustion of solid biomass fuels. Prog Energy Combust Sci 2012;38:113–37.
[11] Schneider T, Krumrein J, Mueller D, Karl J. Investigation of the oxygen supply and distribution in a bubbling fluidized bed by using natural ilmenite for oxygen carrier aided combustion. Energy & Fuels 2021;35:12352–66.
[12] Lind F, Corcoran A, Thunman H. Validation of the oxygen buffering ability of bed materials used for OCAC in a large scale CFB boiler. Powder Technol 2017;316:462–8.
[13] Schneider T, Müller D, Karl J. Effect of natural ilmenite on the solid biomass conversion of inhomogeneous fuels in small-scale bubbling fluidized beds. Energies 2022;15:2747.
[14] Schneider T, Moffitt J, Volz N, Mueller D, Karl J. Long-term effects of ilmenite on a micro-scale bubbling fluidized bed combined heat and power pilot plant for oxygen carrier aided combustion of wood. Appl Energy 2022;314:118953.
[15] Pettersson A, Åmand LE, Steenari BM. Chemical fractionation for the characterisation of fly ashes from co-combustion of biofuels using different methods for alkali reduction. Fuel 2009;88:1758–72.
[16] Tobiasen L, Skytte R, Pedersen LS, Pedersen ST, Lindberg MA. Deposit characteristic after injection of additives to a Danish straw-fired suspension boiler. Fuel Process Technol 2007;88:1108–17.

[17] Lyngfelt A. Chemical-looping combustion of solid fuels - status of development. Appl Energy 2014;113:1869–73.
[18] Hughes RW, Lu DY, Symonds RT. Improvement of oxy-FBC using oxygen carriers: concept and combustion performance. Energy & Fuels 2017;31:10101–15.
[19] Kim SJ, Moon JH, Jo S-H, Park SJ, Kim JY, Beak GU, et al. Enhancing oxygen savings and carbon dioxide purity in biomass oxy-circulating fluidized bed combustion with an oxygen carrier. Fuel 2023;334.
[20] Löffler G, Wargadalam VJ, Winter F. Catalytic effect of biomass ash on CO, CH_4 and HCN oxidation under fluidised bed combustor conditions. Fuel 2002;81:711–7.
[21] Wang XB, Si JP, Tan HZ, Zhao QX, Xu TM. Kinetics investigation on the reduction of NO using straw char based on physicochemical characterization. Bioresour Technol 2011;102:7401–6.
[22] Sun J, Zhao BT, Su YX. Advanced control of NO emission from algal biomass combustion using loaded iron-based additives. Energy 2019;185:229–38.
[23] Faust R, Stanicic I, Gastaldi J, Ansari E, Brorsson J, Mattisson T, et al. Thermodynamic modeling and experimental investigation of the system Fe-Ti-O-K for ilmenite used as fluidized bed oxygen carrier. Energy & Fuels 2024;38:14569–76.
[24] Yang X, Li D, Zhu X, Zhu T, Mun T-Y, Wang H, et al. Interaction of ilmenite oxygen carrier with wheat straw ash during chemical looping combustion: mechanisms and performance variation. Fuel 2024;374.
[25] Corcoran A, Marinkovic J, Lind F, Thunman H, Knutsson P, Seemann M. Ash properties of ilmenite used as bed material for combustion of biomass in a circulating fluidized bed boiler. Energy & Fuels 2014;28:7672–9.
[26] Mack R, Kuptz D, Schoen C, Hartmann H. Combustion behavior and slagging tendencies of kaolin additivated agricultural pellets and of wood-straw pellet blends in a small-scale boiler. Biomass Bioenergy 2019;125:50–62.
[27] Llorente MJF, Arocas PD, Nebot LG, Garcia JEC. The effect of the addition of chemical materials on the sintering of biomass ash. Fuel 2008;87:2651–8.
[28] Luis Miguez J, Porteiro J, Behrendt F, Blanco D, Patino D, Dieguez-Alonso A. Review of the use of additives to mitigate operational problems associated with the combustion of biomass with high content in ash-forming species. Renew Sustain Energy Rev 2021;141:110502.
[29] Kyi S, Chadwick BL. Screening of potential mineral additives for use as fouling preventatives in Victorian brown coal combustion. Fuel 1999;78:845–55.
[30] Thy P, Jenkins BM, Grundvig S, Shiraki R, Lesher CE. High temperature elemental losses and mineralogical changes in common biomass ashes. Fuel 2006;85:783–95.
[31] Thunman H, Lind F, Breitholtz C, Berguerand N, Seemann M. Using an oxygen-carrier as bed material for combustion of biomass in a 12-MW_{th} circulating fluidized-bed boiler. Fuel 2013;113:300–9.
[32] Attah M, Hildor F, Yilmaz D, Leion H. Vanadium recovery from steel converter slag utilised as an oxygen carrier in oxygen carrier aided combustion (OCAC). J Clean Prod 2021;293:126159.
[33] Sun G, Li L, Lu D, Hu M, Sun ZK, Wang RT, et al. Influence of oxygen carrier on NO_x and N_2O emissions in biomass combustion within fluidized beds. Process Saf Environ Prot 2025;193:364–73.
[34] Li L, Sun G, Lu D, Liu H, Liu C, Jin BS, et al. Volatile-N behavior in oxygen carrier aided solid waste combustion using a two-stage fluidized bed reactor. Energy & Fuels 2024;38:21322–32.
[35] Lissianski VV, Maly PM, Zamansky VM, Gardiner WC. Utilization of iron additives for advanced control of NO_x emissions from stationary combustion sources. Ind Eng Chem Res 2001;40:3287–93.
[36] Hayhurst AN, Lawrence AD. The reduction of the nitrogen oxides NO and N_2O to molecular nitrogen in the presence of iron, its oxides, and carbon monoxide in a hot fluidized bed. Combust Flame 1997;110:351–65.
[37] Sun J, Zhao B, Su Y. Advanced control of NO emission from algal biomass combustion using loaded iron-based additives. Energy 2019;185:229–38.
[38] Fu S-L, Song Q, Yao Q. Experimental and kinetic study on the influence of iron oxide on the selective noncatalytic reduction deNO_x process. Ind Eng Chem Res 2014;53:5801–9.
[39] Cao Y, Casenas B, Pan WP. Investigation of chemical looping combustion by solid fuels. 2. Redox reaction kinetics and product characterization with coal, biomass, and solid waste as solid fuels and CuO as an oxygen carrier. Energy & Fuels 2006;20:1845–54.
[40] Zeng L, Cheng Z, Fan JA, Fan LS, Gong JL. Metal oxide redox chemistry for chemical looping processes. Nat Rev Chem 2018;2:349–64.
[41] Sarmiento LEM, Clavier KA, Townsend TG. Trace element release from combustion ash co-disposed with municipal solid waste. Chemosphere 2020;252.
[42] Ke X, Lyu J, Guo X, Shen Z, Zhang M, Zhang Y, et al. Development and application of high-parameter biomass-fired circulating fluidized bed boiler technology. Therm Power Gener 2022;51:1–8.
[43] Hupa M, Karlstrom O, Vainio E. Biomass combustion technology development - it is all about chemical details. Proc Combust Inst 2017;36:113–34.
[44] Reddy BV, Khanna SN. Self-stimulated NO reduction and CO oxidation by iron oxide clusters. Phys Rev Lett 2004;93:068301.
[45] Li J, Zhang Y, Yang H, Yang Y. Study of the effect of ash composition in coal on the kinetic parameters of NO reduction reaction by CO. J China Coal Soc 2016;41:2448–53.
[46] Garcia E, Liu H. Ilmenite as alternative bed material for the combustion of coal and biomass blends in a fluidised bed combustor to improve combustion performance and reduce agglomeration tendency. Energy 2022;239:121913.
[47] Randall H, Doepper R, Renken A. Reduction of nitrogen oxides by carbon monoxide over an iron oxide catalyst under dynamic conditions. Applied Catalysis B-Environmental 1998;17:357–69.
[48] Daood SS, Ord G, Wilkinson T, Nimmo W. Fuel additive technology - NO_x reduction, combustion efficiency and fly ash improvement for coal fired power stations. Fuel 2014;134:293–306.
[49] Ren QQ, Zhao CS, Wu X, Liang C, Chen XP, Shen JZ, et al. Catalytic effects of Fe, Al and Si on the formation of NO_x precursors and HCl during straw pyrolysis. Journal of Thermal Analysis and Calorimetry 2010;99:301–6.
[50] Cheng XX, Wang LY, Wang ZQ, Zhang MZ, Ma CY. Catalytic performance of NO reduction by CO over activated semicoke supported Fe/Co catalysts. Ind Eng Chem Res 2016;55:12710–22.
[51] Rydén M, Hanning M, Lind F. Oxygen carrier aided combustion (OCAC) of wood chips in a 12 MW_{th} circulating fluidized bed boiler using steel converter slag as bed material. Applied Sciences-Basel 2018;8:2657.
[52] Fu SL, Song Q, Yao Q. Experimental and kinetic study on the influence of iron oxide on the selective noncatalytic reduction deNO_x process. Ind Eng Chem Res 2014;53:5801–9.
[53] Ke XW, Engblom M, Yang HR, Brink A, Lyu JF, Zhang M, et al. Prediction and minimization of NO_x emission in a circulating fluidized bed combustor: a comprehensive mathematical model for CFB combustion. Fuel 2022;309.
[54] Ryden M, Hanning M, Corcoran A, Lind F. Oxygen carrier aided combustion (OCAC) of wood chips in a semi-commercial circulating fluidized bed boiler using manganese ore as bed material. Applied Sciences-Basel 2016;6:347.
[55] Li L, Mao J, Tang W, Sun G, Gu Q, Lu X, et al. Experimental study on coal combustion by using the ilmenite ore as active bed material in a 0.3 MWth circulating fluidized bed. Fuel 2023;342.
[56] Johnsson F, Andersson S, Leckner B. Expansion of a freely bubbling fluidized-bed. Powder Technol 1991;68:117–23.
[57] Sit SP, Grace JR. Effect of bubble interaction on interphase mass transfer in gas fluidized beds. Chem Eng Sci 1981;36:327–35.
[58] Scala F. Mass transfer around freely moving active particles in the dense phase of a gas fluidized bed of inert particles. Chem Eng Sci 2007;62:4159–76.
[59] Ke X, Li D, Zhang M, Jeon C-h, Cai R, Cai J, et al. Ash formation characteristics of two Indonesian coals and the change of ash properties with particle size. Fuel Process Technol 2019;186:73–80.